

Tsunami early warning within 5 minutes

Anthony Lomax¹ and Alberto Michelini²

¹ *ALomax Scientific, 161 Allée du Micocoulier, 06370 Mouans-Sartoux, France. e-mail: anthony@alomax.net*

² *Istituto Nazionale di Geofisica e Vulcanologia (INGV), Centro Nazionale Terremoti, Via di Vigna Murata, 605, 00143 Roma, Italy. e-mail: alberto.michelini@ingv.it*

Abbreviated title: Tsunami early warning within 5 minutes

Keywords: Earthquake, Tsunami, Early warning, Earthquake location, Real-time seismology, Body waves.

Submitted to Pure and Applied Geophysics, January 2012; revised May 2012

Abstract

Tsunamis are most destructive at near to regional distances, arriving within 20-30 min after a causative earthquake; effective early warning at these distances requires notification within 15 min or less. The size and impact of a tsunami also depend on sea floor displacement, which is related to the length, L , width, W , mean slip, D , and depth, z , of the earthquake rupture. Currently, the primary seismic discriminant for tsunami potential is the centroid-moment tensor magnitude, M_w^{CMT} , representing the product LWD and estimated through an indirect, inversion procedure. However, the obtained M_w^{CMT} and implied LWD value vary with rupture depth, earth model and other factors, and is only available 20-30 min or more after an earthquake. The use of more direct discriminants for tsunami potential could avoid these problems and aid in effective early warning, especially for near to regional distances.

Previously, we presented a direct procedure for rapid assessment of earthquake tsunami potential using two, simple measures on P -wave seismograms – the predominant period on velocity records, T_d , and the likelihood, T_{50}^{Ex} , that the high-frequency, apparent rupture-duration, T_0 , exceeds 50-55 sec. We have shown that T_d and T_0 are related to the critical rupture parameters L , W , D and z , and that either of the period-duration products $T_d T_0$ or $T_d T_{50}^{\text{Ex}}$ give more information on tsunami impact and size than M_w^{CMT} , M_{wp} and other currently used discriminants. These results imply that tsunami potential is not directly related to the product LWD from the “seismic” faulting model, as is assumed with the use of the M_w^{CMT} discriminant. Instead, information on rupture length, L , and depth, z , as provided by $T_d T_0$ or $T_d T_{50}^{\text{Ex}}$, can constrain well the tsunami potential of an earthquake.

We introduce here special treatment of the signal around the S arrival at close stations, a modified, real-time, $M_{\text{wpd}}(\text{RT})$ magnitude, and other procedures to allow early estimation of event parameters and tsunami discriminants. We show that with real-time data currently available in most regions of tsunami hazard, event locations, m_b and M_{wp} magnitudes and the direct, period-duration discriminant, $T_d T_{50}^{\text{Ex}}$ can be determined within 5 min after an earthquake occurs, and T_0 , $T_d T_0$, and $M_{\text{wpd}}(\text{RT})$ within about 10 min. This processing is implemented and running continuously in real-time within the Early-est earthquake monitor at INGV-Rome (<http://early-est.rm.ingv.it>). We also show that the difference $m_b - \log_{10}(T_d T_0)$ forms a rapid discriminant for slow, tsunami earthquakes. The rapid availability of these

measures can aid in faster and more reliable tsunami early warning for near to regional distances.

Introduction

Tsunamis are most destructive at near to regional distances (e.g. <1000km) of the causative earthquake, arriving within 20-30 min after the earthquake origin time (OT); effective early warning at these distances requires notification within 15 min or less after OT (e.g., Tsushima et al., 2011; Newman et al., 2011; Madlazim, 2011). Currently, rapid assessment of the tsunami potential of an earthquake by organizations such as the Japan Meteorological Agency (JMA), the German-Indonesian tsunami early warning system (GITEWS) or the West Coast and Alaska (WCATWC) and Pacific (PTWC) Tsunami Warning Centers relies mainly on initial estimates of the earthquake location, depth and moment, M_0 , or the corresponding moment magnitude, M_w . For the regional scale, WCATWC and PTWC issue warning messages within about 5-10 min after OT for shallow, underwater events using the P -wave moment-magnitude discriminant, M_{wp} , (Tsuboi *et al.*, 1995; Tsuboi *et al.*, 1999) if $M_{wp} \geq 7.5$ (e.g., Hirshorn and Weinstein, 2009).

M_0 is of interest for tsunami warning because the efficiency of tsunami generation by a shallow earthquake is dependent on the amount of sea floor displacement, which can be related to a finite-faulting model expressed by the seismic potency, LWD , where L is the length, W the width and D the mean slip of the earthquake rupture (e.g., Kanamori, 1972; Abe, 1973; Kajiura, 1981; Lay and Bilek, 2007; Polet and Kanamori, 2009). Then, since $M_0 = \mu LWD$, where μ is the shear modulus at the source, the sea-floor displacement and thus tsunami potential should scale with $LWD = M_0/\mu$.

M_w is found to be a good discriminant for many, past, tsunamigenic earthquakes, but not all, especially not for slow, “tsunami earthquakes” (TsE), which, by definition, cause larger tsunami waves than would be expected from their M_w (e.g., Kanamori, 1972; Satake, 2002; Polet and Kanamori, 2009; Newman et al., 2011). The discrepancy for these earthquakes can be related to rupture at shallow depth where μ can be very low, an-elastic deformation such as ploughing and uplift of sediments may occur, and the fault surface may be non-planar with splay faulting into the accretionary wedge (e.g., Fukao, 1977; Moore *et al.*, 2007; Lay and Bilek, 2007). Additionally, a reliable estimate of M_w for large earthquakes is usually provided by a centroid-moment tensor magnitude, M_w^{CMT} , (Dziewonski *et al.*, 1981; Ekström *et al.*, 2005), which requires waveform inversion, varies with rupture depth, earth model and other factors, and is only available 20-30 min or more after an earthquake (e.g. Hayes et al., 2011; Duputel et al., 2011). Thus rapid magnitude estimators such as M_{wp} are used for tsunami warning, but M_{wp} performs poorly relative to M_w^{CMT} and other discriminants for tsunami potential (Lomax and Michelini, 2011A, LM2011 hereinafter).

To avoid these problems and aid in effective early warning, especially for near to regional distances, we suggest the use of more direct and rapid discriminants for tsunami potential and for identification of TsE's. We have presented (Lomax and Michelini, 2009B; LM2011; Lomax and Michelini, 2011B) a direct procedure for rapid assessment of earthquake tsunami potential using two, simple measures on P -wave seismograms – the predominant period on velocity records, T_d , and the likelihood, T_{50}^{Ex} , that the high-frequency, apparent rupture-duration, T_0 , exceeds 50-55 sec. T_0 for large earthquakes is related primarily to rupture length, L , and both T_d and T_0 will increase as rupture depth, z , decreases, due to the effects of a reduced shear modulus and rupture velocity, v_r . We show in LM2011 that either of the period-duration products $T_d T_0$ or $T_d T_{50}^{Ex}$ give more information on tsunami impact and size than M_w^{CMT} , M_{wp} , M_{wpd} (Lomax and Michelini, 2009A, LM2009A hereinafter), and other currently used discriminants. These results imply that tsunami potential is not directly related to the product LWD from the “seismic” faulting model, as is assumed with the use of M_w

discriminants, and suggest instead that information on rupture length and depth can constrain well the tsunami potential of an earthquake. This information on rupture length and depth is provided by $T_d T_0$ and $T_d T_{50}^{\text{Ex}}$, in which case explicit estimates of rupture length and depth, which are difficult to impossible to determine rapidly, are not required.

Effectively, as shown schematically in Figure 1, for a fault of fixed potency LWD , as rupture depth decreases the quantity $T_d T_0$ increases, reflecting the increased tsunami potential of the shallowest, underwater earthquakes, including TsE's. This behaviour suggests that the $T_d T_0$ discriminant captures the “tsunami” faulting model corresponding to the observed tsunami waves (Satake, 1994), as opposed to the “seismic” faulting model as given by M_0 . In this case $T_d T_0$ may also be a valuable aid in defining the finite-faulting description of the source and sea floor displacement for real-time tsunami forecasting.

We introduce here special treatment of the signal around the S arrival at close stations, a modified, real-time, M_{wpd} magnitude ($M_{\text{wpd}}(\text{RT})$), and other procedures to allow early estimation of multiple event parameters. We show that, with current, real-time seismogram data, rapid calculation of the direct, period-duration discriminant, $T_d T_{50}^{\text{Ex}}$, can be completed within 5 min after OT, and calculation of T_0 , $T_d T_0$, and $M_{\text{wpd}}(\text{RT})$ magnitudes within about 10 min. We also show that the difference $m_b - \log_{10}(T_d T_0)$ forms a useful, rapid discriminant for TsE's. We illustrate that the rapid availability of these measures can aid in faster and more reliable tsunami early warning for near to regional distances.

Rapid, direct assessment of tsunami potential

To rapidly assess T_0 for an earthquake we use the duration-exceedance (DE) procedure of Lomax and Michelini (2009B) which, through analysis of high-frequency (HF), vertical-component seismograms, determines if T_0 for an earthquake is likely to exceed 50-55s (Figure 2). On 1-5 Hz band-pass filtered seismogram we form the ratio of the *rms* amplitude, A_{50} , from 50-60 s after the P arrival time, T_p , with the *rms* amplitude, A_{25} , for the first 25 s after T_p to obtain a station DE level, $l_{50} = A_{50}/A_{25}$, available about 60 s after T_p . We define an event DE level, T_{50}^{Ex} , as the median of the station l_{50} values. If T_{50}^{Ex} is greater (less) than 1.0, then T_0 is likely (unlikely) to exceed 50-55 s.

We define the dominant period, T_d , for an event as the median of the dominant period values for each station given by the peak of the τ_c algorithm (Nakamura, 1988; Wu and Kanamori, 2005) applied with a 5 s sliding time-window from 0 to 55 s after the P arrival on velocity seismograms (Figure 2; LM2011). Then, taking T_{50}^{Ex} as a substitute for T_0 , the $T_d T_0$ discriminant for tsunami potential becomes $T_d T_{50}^{\text{Ex}}$ (i.e., $T_d T_{50}^{\text{Ex}} \geq 8.0$ s).

To enable calculation of $T_d T_{50}^{\text{Ex}}$, T_0 , m_b , M_{wp} and M_{wpd} within 5 min after an earthquake occurs we modify the procedures described in LM2011, including reduction of the minimum station distance to 5° for all measures, and special treatment of the signal around the S arrival time, T_s , at close stations:

1. For distances less than 30° significant S signal may remain on the HF seismograms (LM2009A). Consequently, if the raw, HF duration (T_0^{raw}) determined following LM2011 ends later than $(T_s - T_p)/4$ after T_s , we assume that the HF signal after T_s is primarily S wave energy, and that a best estimate of T_0 is measured starting at T_s . That is, if $T_0^{\text{raw}} > (T_s - T_p) + (T_s - T_p)/4$ then $T_0 = T_0^{\text{raw}} - (T_s - T_p)$, (Figure 2).
2. To prevent including S energy in the magnitude estimates, the M_{wp} and M_{wpd} analysis windows are truncated at T_s .

Additionally we modify M_{wpd} from the formulation of LM2009A to allow simple and robust real-time application without event type determination by:

1. using the M_{wp} constant $4\pi\rho\alpha^3 r/F^p$ from Tusboi et al. (1995, 1999), where ρ is density, α

is P velocity, r is station-source distance and F^P a radiation pattern correction,

2. applying the depth correction but no other geometrical or attenuation corrections from LM2009A, and
3. applying the moment correction of LM2009A to all event types if $T_0 > 90$ s; to prevent discontinuous jumps in magnitude, this correction is applied using a linear-ramp, weight factor from 0 at 90s to 1.0 at and above 110s.

We identify this magnitude as $M_{\text{wpd}}(\text{RT})$.

We also calculate m_b on simulated WWSSN-SP velocity traces following the V_{max} procedure of Bormann and Saul (2008), we identify this magnitude as $m_b(V_{\text{max}})$.

The processing procedures discussed here are implemented and running continuously in real-time within the Early-est software and earthquake monitor at INGV-Rome (<http://early-est.rm.ingv.it>), including rapid calculation of event locations, $T_d T_{50}^{\text{Ex}}$ and $m_b(V_{\text{max}})$ and M_{wp} magnitudes within around 5 min, and T_0 , $T_d T_0$, $M_{\text{wpd}}(\text{RT})$ magnitudes and P first-motion, fault-plane solutions within about 10 min.

Application to recent large earthquakes

We consider a reference set of 120 large earthquakes ($6.4 \geq M_w \geq 9.1$; 103 shallow, under water) since 1992, when high-quality, broadband seismograms became widely available, along with measures of the impact and size of any generated tsunamis (Table S1). This reference set includes most tsunamigenic earthquakes listed in the NOAA/WDC Historical Tsunami Database (http://www.ngdc.noaa.gov/hazard/tsu_db.shtml), most events of $M_w \geq 7$ in the past few years and several events of regional importance.

As a measure of tsunami impact we define an approximate measure of tsunami importance, I_t , for the reference earthquakes based on 0-4 descriptive indices of tsunami effects and maximum water height h in meters from the NOAA/WDC database (see LM2011 for details). I_t is approximate since it depends strongly on the available instrumentation, coastal bathymetry and population density in the event region. $I_t \geq 2$ corresponds approximately to the JMA threshold for issuing a ‘‘Tsunami Warning’’; the largest or most devastating tsunamis typically have $I_t \geq 10$.

Using the Early-est software and off-line, event data from available stations, we determine event locations, $m_b(V_{\text{max}})$, M_{wp} , $M_{\text{wpd}}(\text{RT})$, T_0 , $T_d T_0$ and $T_d T_{50}^{\text{Ex}}$ for the reference earthquakes at OT+5 min to simulate the information available within 5 min after an earthquake occurs, and at OT+15 min to simulate the near final values of the event parameters. These delay times do not include real-time data transmission and processing latencies, which are currently typically less than 1 min. Figure 3 shows a comparison of M_w^{CMT} , M_{wp} and $T_d T_0$ with I_t for the reference earthquakes at OT+15 min; Table 1 shows summary results for all discriminants at OT+15 min or later (M_w^{CMT}), and for T_{50}^{Ex} and $T_d T_{50}^{\text{Ex}}$ at OT+5 min; Table S1 lists complete results for all events at OT+15 min. Figure 3 also shows that $M_{\text{wpd}}(\text{RT})$ compares well with final M_w^{CMT} for the studied earthquakes, justifying the real-time modifications to M_{wpd} presented above.

For the reference events, the period-duration discriminant $T_d T_0$ shows a better correspondence with I_t than either M_w^{CMT} or M_{wp} (Figure 3). At OT+15 min both $T_d T_0$ and $T_d T_{50}^{\text{Ex}}$ correctly identify 72-74% of tsunamigenic events with $I_t \geq 2$ (Table 1), more than the M_{wp} (44%), M_w^{CMT} (68%) and T_0 (68%) discriminants, with fewer false positive identifications of events with $I_t < 2$. All discriminants are poor at identifying the tsunami potential of oceanic, strike-slip events, and give mixed results for back-arc intraplate earthquakes (see LM2011 for details). At OT+5 min, with fewer available events (due to lack of data, mainly for earlier events), the $T_d T_{50}^{\text{Ex}}$ discriminant shows about the same rate of correct classification of events as at OT+15 min. These results show that use of the $T_d T_{50}^{\text{Ex}}$ discriminant for tsunami potential at OT+5

min and perhaps earlier should be reliable and useful, especially as more real-time stations become available in regions of high tsunami hazard.

In LM2011 the tsunami discriminants are also compared using a physical measure of tsunami size - a tsunami wave amplitude at 100km distance from the source, A_t , estimated from water height data in the NOAA/WDC database. As above for tsunami impact, I_t , comparisons in LM2011 shows that T_dT_0 or $T_dT_{50}^{\text{Ex}}$ give more information on tsunami size, A_t , than M_w^{CMT} , M_{wp} and other currently used discriminants (Table S1). Moreover, there is indication of a linear, and thus possibly a physical, relationship between $\log(T_dT_0)$ and A_t .

The results for the reference events also show that the difference $m_b - \log_{10}(T_dT_0) < \sim 3.2$ forms a useful discriminant for TsE's (Figure 5; Table S1). This difference relationship is related to the energy-to-moment parameter, Θ , (Newman and Okal, 1998; Weinstein and Okal, 2005) and to recent, rapid, energy- and moment- to-duration discriminants for TsE's (e.g. Lomax et al, 2007; LM2009A; Newman et al., 2011). In addition to previously identified TsE's, preliminary results for this discriminant suggest a strong component of TsE for other events, including the $M_w7.0$, 1998.07.17 Papua New Guinea earthquake and the $M_w8.1$, 2007.04.01 and $M_w7.0$, 2010.01.03 Solomon Islands earthquakes, all of which were strongly tsunamigenic (Table S1). Since the relationship $m_b - \log_{10}(T_dT_0)$ can be evaluated rapidly ($m_b(V_{\text{max}})$ is available a few minutes after OT while T_dT_0 is typically available before OT+10 min), further investigation of this difference relationship is warranted, perhaps with m_b replaced by a mean of HF amplitude, or an energy integral, from T_P to T_P+T_0 .

Example timelines for assessment of tsunami potential

We simulate and examine detailed timelines for event characterisation and assessment of tsunami potential using the Early-est software and off-line, event data for several events: an earthquake that produced a mild tsunami, 2009.03.19, $M_w^{\text{CMT}} 7.6$, Tonga (Figure 5), and two earthquakes that produced large tsunamis, the 2011.03.11, $M_w^{\text{CMT}} 9.1$, Tohoku, Honshu, Japan mega-quake (Figure 6) and the 2010.10.25, $M_w^{\text{CMT}} 7.8$, Mentawai, Sumatra, Indonesia TsE (Figure 7).

For the 2009 Tonga event the PTWC (2009) issued a tsunami warning at OT+12 min based on a magnitude measure of $M 7.7$; the tsunami warning was cancelled 1.5 hours later. This earthquake generated a mild, non-destructive tsunami with observed water heights mostly less than 0.1 m (NOAA/WDC database). For this event (Figure 5), Early-est determines at OT+4→5 min the epicentre with an error of about 35 km, along with $M_{\text{wp}} 7.6$ and at OT+7 min $M_{\text{wpd}}(\text{RT}) 7.7$, both in good agreement with the final M_w^{CMT} . At OT+5→7 min, all three discriminant for tsunami potential, $T_dT_{50}^{\text{Ex}}$, T_0 and T_dT_0 are available and indicate a low tsunami potential for this event. All Early-est measures have stabilized to near-final values within OT+8→10 min.

For the devastating 2011 Tohoku earthquake and tsunami JMA first issued a tsunami warning at about OT+3 min, but a near-final M_w and the true size of this event were not determined until OT+20→30 min (Ozaki, 2011; Hayes et al., 2011). For this earthquake (Figure 6), Early-est determines the epicentre at OT+2→3 min with an error of about 60 km, $M_{\text{wp}} 8.0-8.3$ at OT+4→6 min, and $M_{\text{wpd}}(\text{RT}) 9.0-9.2$ at OT+6→8 min. These epicentre and M_{wp} results compare favourably with the JMA and NEIC response timelines (Ozaki, 2011; Hayes et al., 2011), while the near-final $M_{\text{wpd}}(\text{RT})$ determination precedes the earliest M_w^{CMT} estimation (NEIC M_{ww}) by about 12 min. The $T_dT_{50}^{\text{Ex}}$ discriminant for tsunami potential is available at OT+4→5 min and the T_0 and T_dT_0 measures are available at OT+6→7 min; all three of these discriminants indicate a very high likelihood that a tsunami was generated. Almost all Early-est measures have stabilized to near-final values within OT+7→8 min, one exception being epicentre which only stabilizes at OT+9→10 min due to the lack of station coverage off-shore to the east of the epicentre. For this event it is notable that the $M_{\text{wpd}}(\text{RT}) 9.2$ magnitude and

$T_0=160$ s duration estimates provide early information on the true size and extent of the earthquake rupture and tsunami source; these rapid measures should be useful during future large earthquakes not only for tsunami warning, but also for early shake-map, finite-fault and tsunami forecast modelling.

The 2010 Mentawai earthquake generated a large and destructive, local tsunami and has been identified as a TsE (Newman et al., 2011; Madlazim, 2011). The timeline for Early-est characterization of this event (Figure 7) is similar to that for 2011 Tohoku, except that the M_{wp} , M_{wpd} (RT) and $T_d T_{50}^{Ex}$ measures are available about 1 min earlier, at OT+3→4 min, and the epicentre is better constrained in the first minutes. These differences are mainly due to denser station coverage near this event, though there is still a lack of stations off-shore to the southwest of the epicentre. All three discriminant for tsunami potential, $T_d T_{50}^{Ex}$ at OT+3→4 min, and T_0 and $T_d T_0$ at OT+5→6 min, indicate a high likelihood that a tsunami was generated. All measures have stabilized to near their final values within OT+7→8 min, though the large, early values for $T_d T_{50}^{Ex}$ indicate that the determination of this measure for near stations might be improved. For this event, in addition to early indication of high tsunami potential at OT+3→6 min, Early-est gives at OT+6→9 min a stable M_{wpd} (RT) 7.8-7.9 that matches final M_w^{CMT} , and $m_b - \log_{10}(T_d T_0) \approx 3.0$, suggesting this event is a TsE.

Conclusions

We have presented rapid determination of tsunami potential using two, direct and simple measures on P -wave seismograms, the predominant period, T_d , and the likelihood, T_{50}^{Ex} , that the T_0 , exceeds 50-55 sec (LM2011). We have also introduced a modified, real-time, M_{wpd} (RT) magnitude, and special treatment of the signal around the S arrival at close stations to allow early estimation of all event parameters. We find that either of the period-duration products $T_d T_0$ or $T_d T_{50}^{Ex}$ give more information on tsunami impact and size than M_w^{CMT} , M_{wp} and other currently used discriminants. This result follows from T_0 and T_d being most sensitive to rupture length, L , and depth, z , which control total seafloor uplift and tsunami potential.

We show that the $T_d T_{50}^{Ex}$ discriminant can be obtained within 5 min after an earthquake occurs with real-time data currently available in most regions of tsunami hazard. We also show that other critical event parameters can be obtained within 5-10 min, including: the T_0 and $T_d T_0$ tsunami potential discriminants, an M_{wpd} (RT) that matches closely final M_w^{CMT} , and the difference $m_b - \log_{10}(T_d T_0)$ which forms a rapid discriminant for slow, tsunami earthquakes. The rapid availability of these direct and simple measures can aid in faster and more reliable tsunami early warning for near to regional distances.

Acknowledgements

We thank two reviewers for critical comments that greatly improved the clarity of the manuscript. This work is supported by INGV - Centro Nazionale Terremoti institutional funds and by the EC n.262330 NERA 2010-2014 project. The IRIS DMC (<http://www.iris.edu>) and GFZ Data Archive (<http://geofon.gfz-potsdam.de>) provided access to waveforms used in this study.

References

- Abe, K. (1973), Tsunami and mechanism of great earthquakes, *Phys. Earth Planet. Int.*, 7, 143-153.
- Bormann, P., and Saul, J. (2008), The new IASPEI standard broadband magnitude mB. *Seis. Res. Lett.*, 79(5), 698–705; doi: 10.1785/gssrl.80.5.698

- Dziewonski, A., Chou, T.A., and Woodhouse, J. H. (1981), Determination of earthquake source parameters from waveform data for studies of global and regional seismicity, *J. Geophys. Res.*, *86*, 2825-2852.
- Duputel, Z., Rivera, L., Kanamori, H., Hayes, G.P., Hirshorn, B., and Weinstein, S. (2011), Real-time W phase inversion during the 2011 off the Pacific coast of Tohoku Earthquake, *Earth Planets Space*, *63*(7), 535-539.
- Ekström, G., Dziewonski, A.M., Maternovskaya, N.N., and Nettles, M. (2005), Global seismicity of 2003: Centroid-moment-tensor solutions for 1087 earthquakes, *Phys. Earth Planet. Inter.*, *148*, 327– 351.
- Fukao, Y. (1979), Tsunami Earthquakes and Subduction Processes Near Deep - Sea Trenches, *J. Geophys. Res.*, *84*, 2303-2314.
- Hayes, G.P., Earle, P.S., Benz, H.M., Wald, D.J., Briggs, R.W., and the USGS/NEIC Earthquake Response Team (2011), 88 Hours: The U.S. Geological Survey National Earthquake Information Center Response to the 11 March 2011 Mw 9.0 Tohoku Earthquake, *Seis. Res. Lett.*, *82*, 481-493, doi: 10.1785/gssrl.82.4.481
- Hirshorn, B., and Weinstein, S. (2009), Earthquake Source Parameters, Rapid Estimates for Tsunami Warning, in *Encyclopedia of Complexity and Systems Science*, edited by A. Meyers, Springer, New York, 10370pp., doi:10.1007/978-0-387-30440-3_160
- Kanamori, H. (1972), Mechanism of tsunami earthquakes, *Phys. Earth Planet. Int.*, *6*, 246 - 259.
- Kajiura, K. (1981), Tsunami energy in relation to parameters of the earthquake fault model, *Bulletin of the Earthquake Research Institute*, *56*, 415–440.
- Lay, T., and Bilek, S. (2007), Anomalous earthquake ruptures at shallow depths on subduction zone megathrusts, in *The Seismogenic Zone of Subduction Thrust Faults*, edited by T. H. Dixon and C. Moore, Columbia Univ. Press, New York, 692pp, ISBN: 978-0-231-13866-6.
- Lomax, A., Michélini, A. and Piatanesi, A. (2007), An energy-duration procedure for rapid determination of earthquake magnitude and tsunamigenic potential, *Geophys. J. Int.*, *170*, 1195-1209, doi:10.1111/j.1365-246X.2007.03469.x
- Lomax, A. and Michélini, A. (2009A), M_{wpd} : A duration-amplitude procedure for rapid determination of earthquake magnitude and tsunamigenic potential from *P* waveforms, *Geophys. J. Int.*, *176*, 200–214, doi:10.1111/j.1365-246X.2008.03974.x
- Lomax, A. and Michélini, A. (2009B), Tsunami early warning using earthquake rupture duration, *Geophys. Res. Lett.*, *36*, L09306, doi:10.1029/2009GL037223
- Lomax, A. and Michélini, A. (2011A), Tsunami early warning using earthquake rupture duration and *P*-wave dominant period: the importance of length and depth of faulting, *Geophys. J. Int.*, *185*, 283–291, doi: 10.1111/j.1365-246X.2010.04916.x
- Lomax, A. and Michélini, A. (2011B), Erratum, *Geophys. J. Int.*, *186*, 1454, doi: 10.1111/j.1365-246X.2011.05128.x
- Madlazim (2011), Toward Indonesian Tsunami Early Warning System by Using Rapid Rupture Durations Calculation, *Science of Tsunami Hazards*, *30*(4)4, 233-243.
- Moore, G. F., Bangs, N. L., Taira, A., Kuramoto, S., Pangborn, E., Tobin, H. J. (2007), Three-Dimensional Splay Fault Geometry and Implications for Tsunami Generation. *Science* *318*, 1128, DOI: 10.1126/science.1147195
- Nakamura, Y. (1988), On the urgent earthquake detection and alarm system (UrEDAS), *Proc.*

of the 9th World Conference on Earthquake Engineering, Tokyo-Kyoto, Japan.

- Newman, A.V., and Okal, E.A. (1998), Teleseismic Estimates of Radiated Seismic Energy: The E/M_0 Discriminant for Tsunami Earthquakes, *J. Geophys. Res.*, **103** (11), 26,885-98.
- Newman, A.V., Hayes, G., Wei, Y., and Convers, J. (2011), The 25 October 2010 Mentawai tsunami earthquake, from real-time discriminants, finite-fault rupture, and tsunami excitation, *Geophys. Res. Lett.*, **38**, L05302, doi:10.1029/2010GL046498.
- Ozaki, T. (2011), Outline of the 2011 off the Pacific coast of Tohoku Earthquake (Mw 9.0) - Tsunami warnings/advisories and observations, *Earth Planets Space*, **63**, 827–830, doi:10.5047/eps.2011.06.029
- Polet, J., and Kanamori, H. (2009), Tsunami Earthquakes, in *Encyclopedia of Complexity and Systems Science*, edited by A. Meyers, Springer, New York, 10370pp., doi:10.1007/978-0-387-30440-3_567
- PTWC (2009), Tsunami Bulletin Number 001, issued at 1830Z 19 MAR 2009, Pacific Tsunami Warning Center/NOAA/NWS.
- Satake, K. (1994), Mechanism of the 1992 Nicaragua Tsunami Earthquake, *Geophys. Res. Lett.*, **21**(23), 2519–2522.
- Satake, K. (2002), Tsunamis, in *International Handbook of Earthquake and Engineering Seismology*, pp. 437–451, eds W.H.K. Lee, H. Kanamori, P.C. Jennings & C. Kisslinger, Academic Press, Amsterdam.
- Tsuboi, S., Abe, K., Takano, K., and Yamanaka, Y. (1995), Rapid determination of M_w from broadband P waveforms, *Bull. Seism. Soc. Am.*, **85**, 606-613.
- Tsuboi, S., Whitmore, P. M., and Sokolowski, T. J. (1999), Application of M_{wp} to deep and teleseismic earthquakes, *Bull. Seism. Soc. Am.*, **89**, 1345-1351.
- Tsushima, H., Hirata, K., Hayashi, Y., Tanioka, Y., Kimura, K., Sakai, S., Shinohara, M., Kanazawa, T., Hino, R., and Maeda, K. (2011), Near-field tsunami forecasting using offshore tsunami data from the 2011 off the Pacific coast of Tohoku Earthquake, *Earth Planets Space*, **63**, 821–826.
- Weinstein, S.A., and Okal, E.A. (2005), The mantle wave magnitude M_m and the slowness parameter θ : Five years of real-time use in the context of tsunami warning, *Bull. Seism. Soc. Am.*, **95**, 779-799.
- Wu, Y-M., and Kanamori, H. (2005), Experiment on an onsite early warning method for the Taiwan early warning system, *Bull. Seism. Soc. Am.*, **95**, 347-353.

Table 1. Tsunami discrimination results

Discriminant	Available (min after OT)	Critical Value	Correctly Identified			Missed	False
			$I_t \geq 2$	%*	$I_t < 2$	$I_t \geq 2$	$I_t < 2$
M_w^{CMT} (Final)**	20+	7.45	34	68%	41	16	13
Results at OT+15 min**							
M_{wp}	3-10	7.45	22	44%	45	28	9
M_{wpd} (RT)	6-10	7.45	38	76%	37	12	17
T_0	6-10	5.5	34	68%	41	16	13
$T_d T_0$	6-10	5.10	36	72%	44	14	10
T_{50}^{Ex}	4-8	1.0	31	62%	48	19	6
$T_d T_{50}^{Ex}$	4-8	8.0	37	74%	45	13	9
Results at OT+5 min***							
T_{50}^{Ex}	4-8	1.0	17	81%	20	4	9
$T_d T_{50}^{Ex}$	4-8	8.0	17	81%	20	4	9

* percent of all events with $I_t \geq 2$ that are correctly identified

** 104 events classified; 50 have $I_t \geq 2$

*** 50 events classified; 21 have $I_t \geq 2$

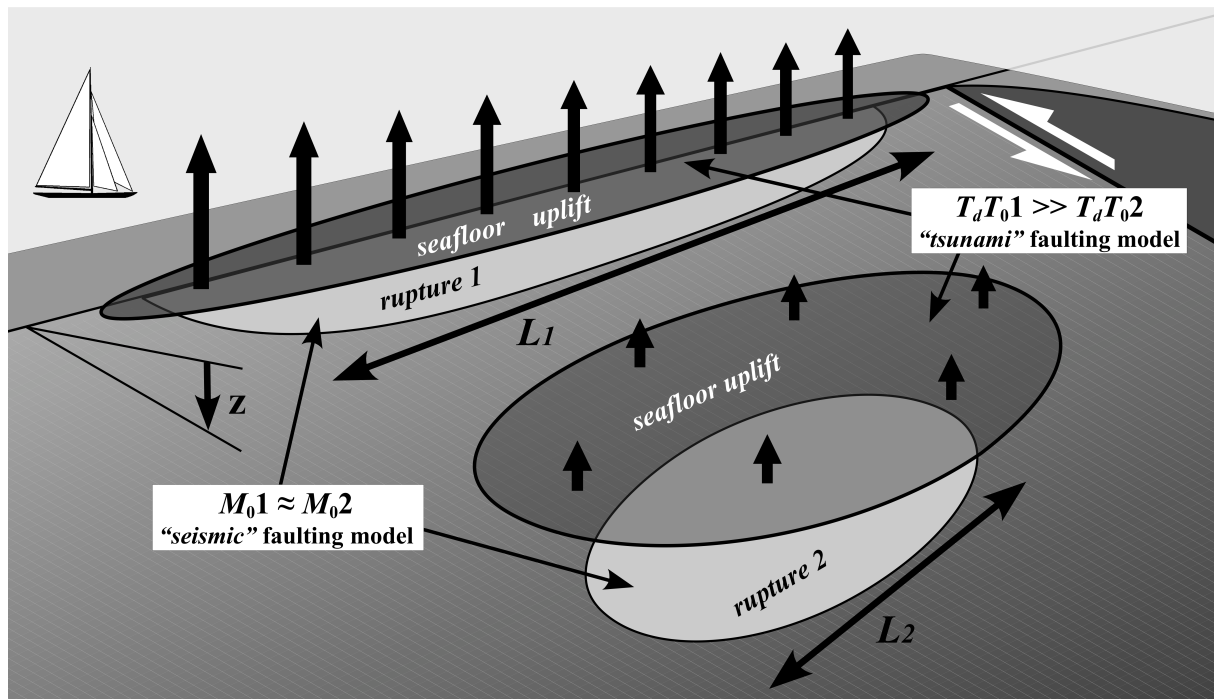


Figure 1

Simplified diagram of a subduction zone mega-thrust showing two interplate thrust ruptures 1 and 2 with the same seismic potency LWD (light grey patches), but different vertical seafloor displacement (uplift areas shown in dark grey). The long, shallow rupture 1 produces greater total seafloor uplift than the deeper rupture 2. Since $M_0 = \mu LWD$ and μ increases with depth, M_0 , the “seismic” faulting model, will be smaller for rupture 1 than for rupture 2. In contrast, since $L_1 > L_2$, and the rupture velocity, v_r , is lower at shallow depths, $T_0 \propto L/v_r$ will be larger for rupture 1 than for rupture 2. Since T_d may give additional information on z , W or D , the quantities $T_d T_0$ and $T_d T_{50}^{Ex}$ for rupture 1 can be larger or much larger than for rupture 2, reflecting the “tsunami” faulting model and correctly identifying the greater seafloor uplift and tsunami potential of the long, shallow rupture 1.

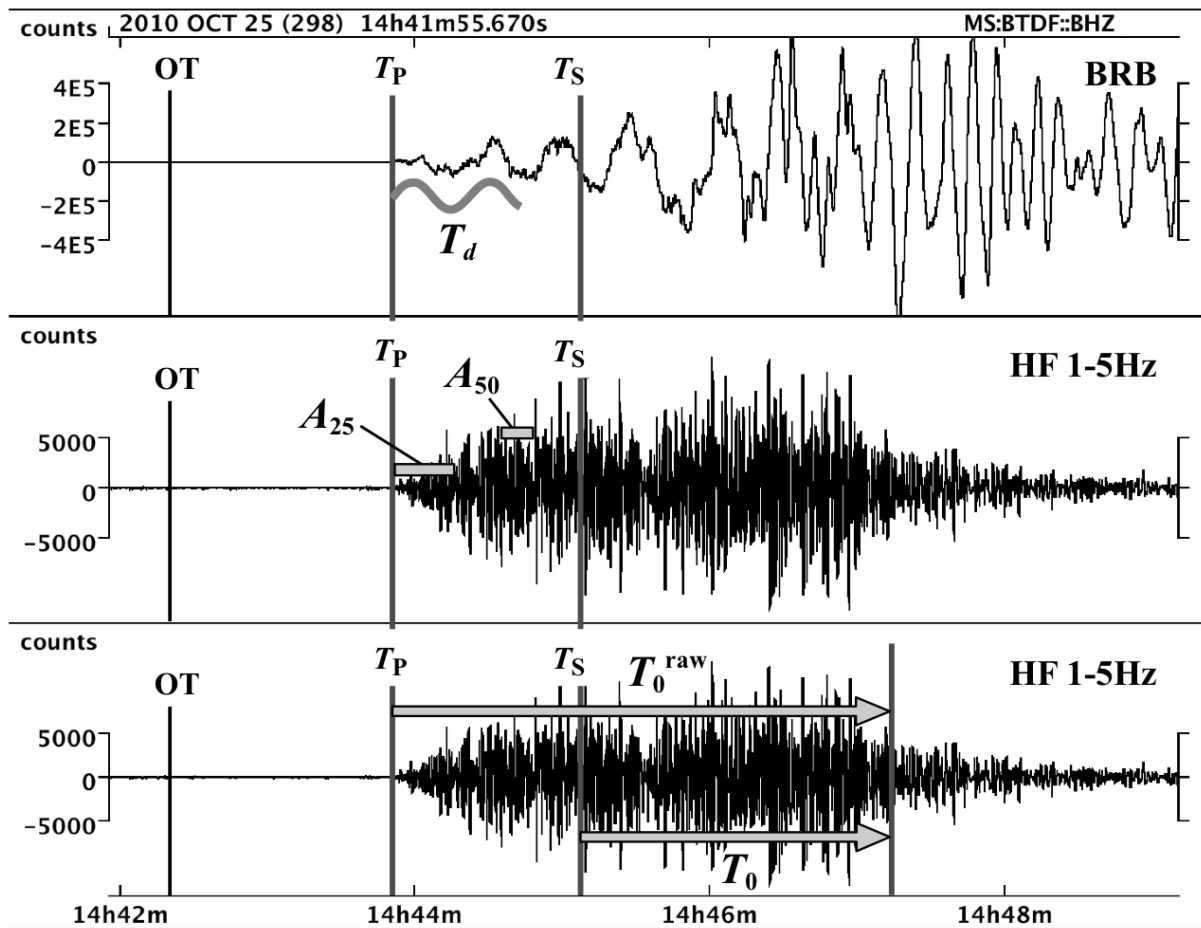


Figure 2

Schematic of single-station, period-duration processing for the 2010.10.25, M_w 7.8, Mentawai earthquake at station MS.BTDF at 6° GCD. (top trace) raw, broadband velocity with T_d period estimation. (middle trace) HF seismogram showing estimation of the station DE level, $I_{50}=A_{50}/A_{25}$. (bottom trace) HF seismogram showing estimation of T_0 when T_0^{raw} ends after T_s .

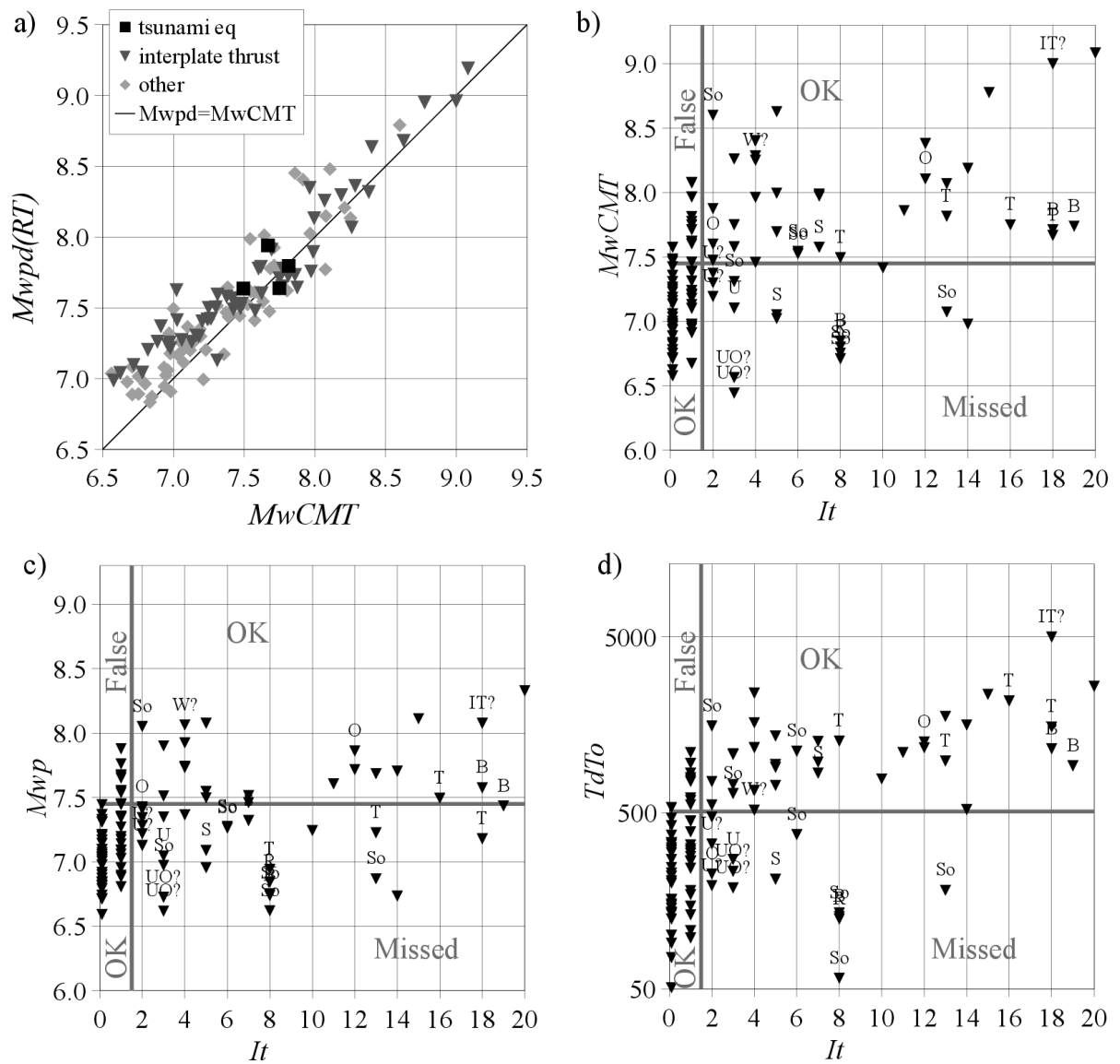


Figure 3

Processing results for the studied events. a) $M_{wpd}(RT)$, modified for real-time application and evaluated at OT+15 min, compared to final M_w^{CMT} . b-d) Comparison of tsunami importance, I_t , with b) final M_w^{CMT} , c) M_{wp} at OT+15 min, and d) $T_d T_0$ at OT+15 min. Vertical grey lines show the target $I_t \geq 2$ threshold; horizontal grey lines show the critical values for each discriminant (Table 1). The $T_d T_0$ axis uses logarithmic scaling. Event labels show earthquakes type for non interplate-thrust events with $I_t \geq 2$ (I -interplate-thrust; T -tsunami earthquake; O -outer-rise intraplate; B -back-arc intraplate; U -upper-plate intraplate; So -strike-slip oceanic, S -strike-slip continental, R -reverse-faulting).

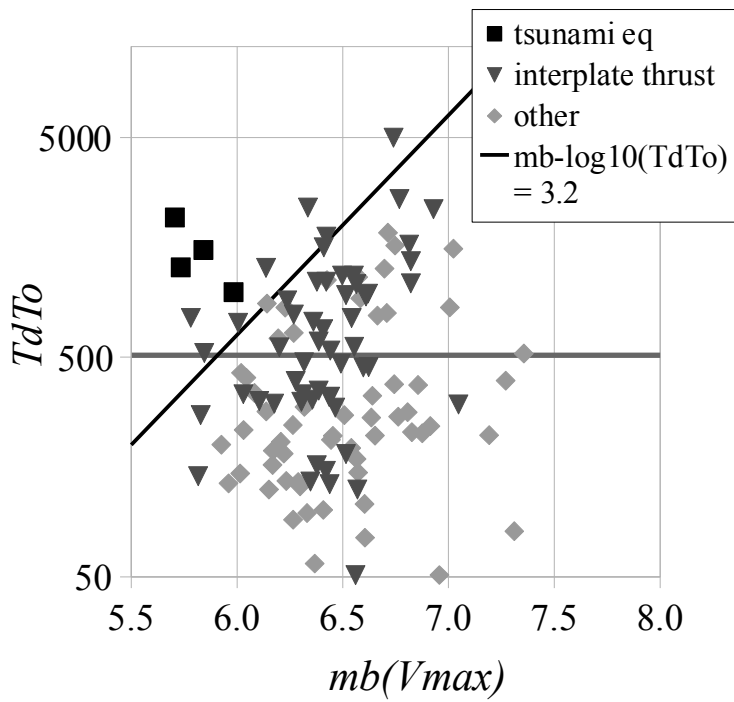


Figure 4

$m_b(V_{max})$ compared to $T_d T_0$, both evaluated at OT+15 min (see also Table S1). The $T_d T_0$ axis uses logarithmic scaling. The horizontal grey line show the critical value for the $T_d T_0$ discriminant (Table 1); the diagonal line shows the constant difference $m_b - \log_{10}(T_d T_0) = 3.2$.

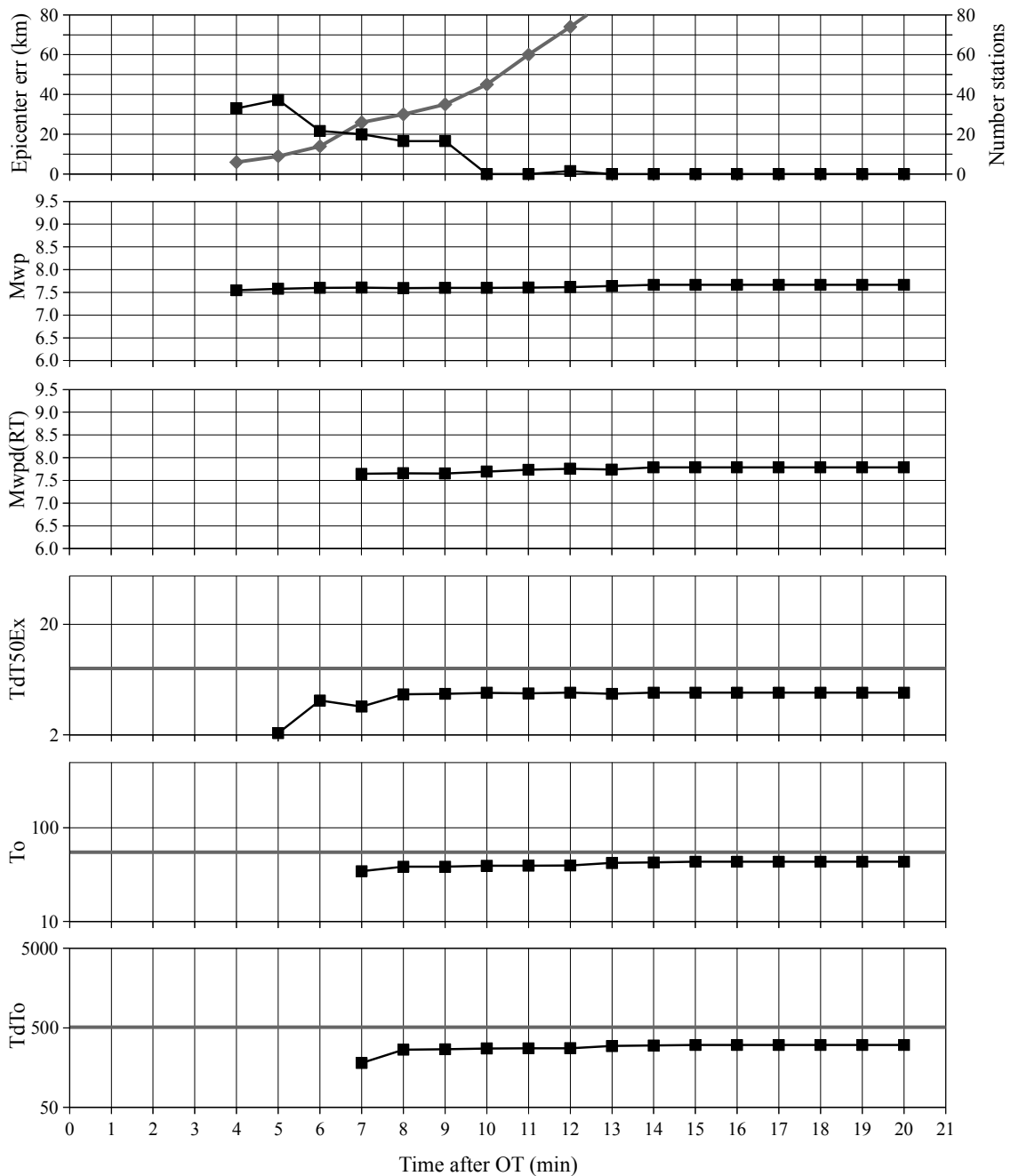


Figure 5

Timeline of event parameter determination for the 2009.03.19, M_w^{CMT} 7.6, Tonga earthquake using the Early-est software and off-line event data. The top panel shows (black curve) epicentre location error relative to the final epicentre and (grey curve) the number of stations used for location. The remaining panels show the main magnitude and tsunamigenic discriminants discussed in this paper. Horizontal grey lines show the critical values for the $T_dT_{50}^{Ex}$, T_0 and T_dT_0 discriminants (Table 1).

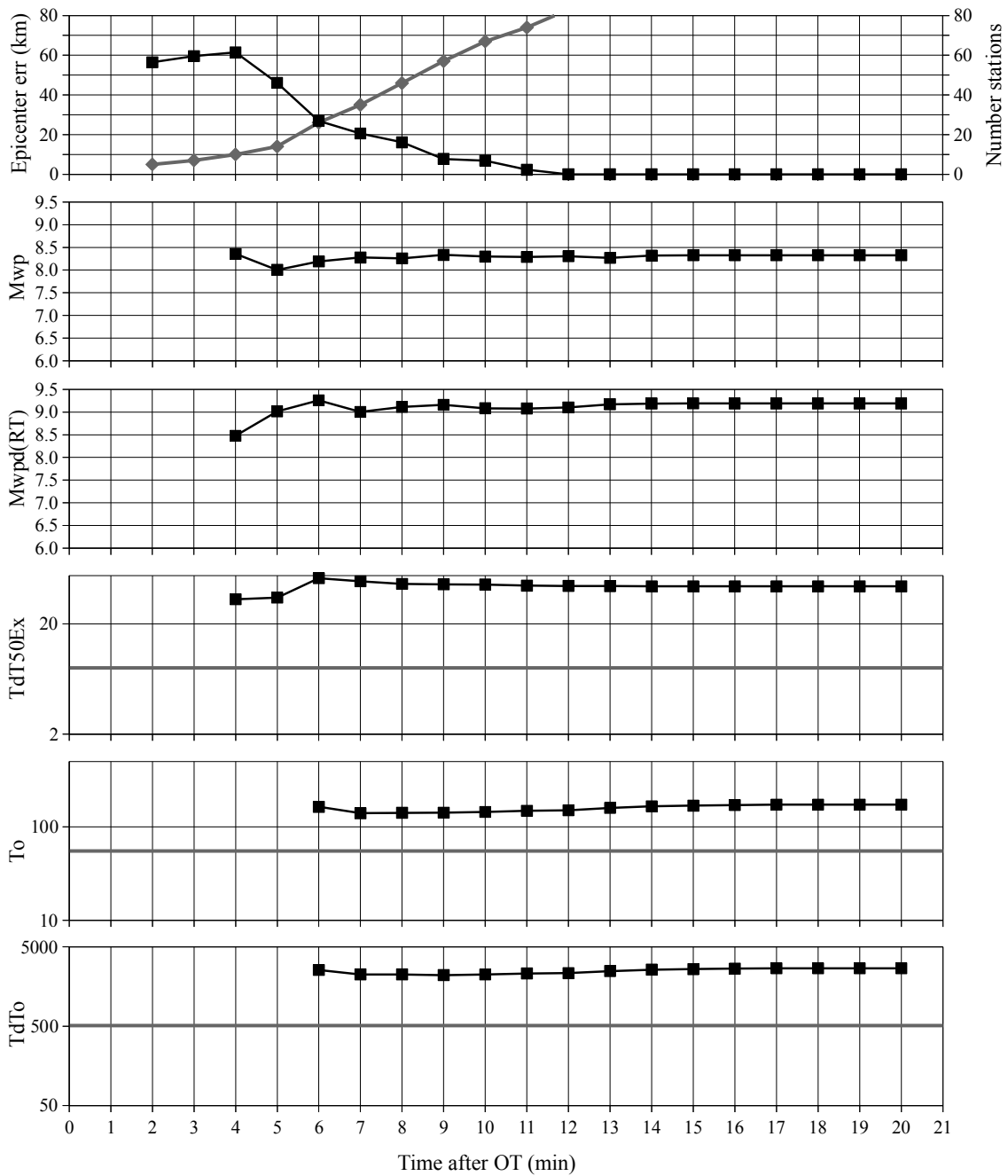


Figure 6

Timeline of event parameter determination for the 2011.03.11, $M_w^{CMT} 9.1$, Tohoku, Japan earthquake using the Early-est software and off-line event data. Plot elements as in Figure 5.

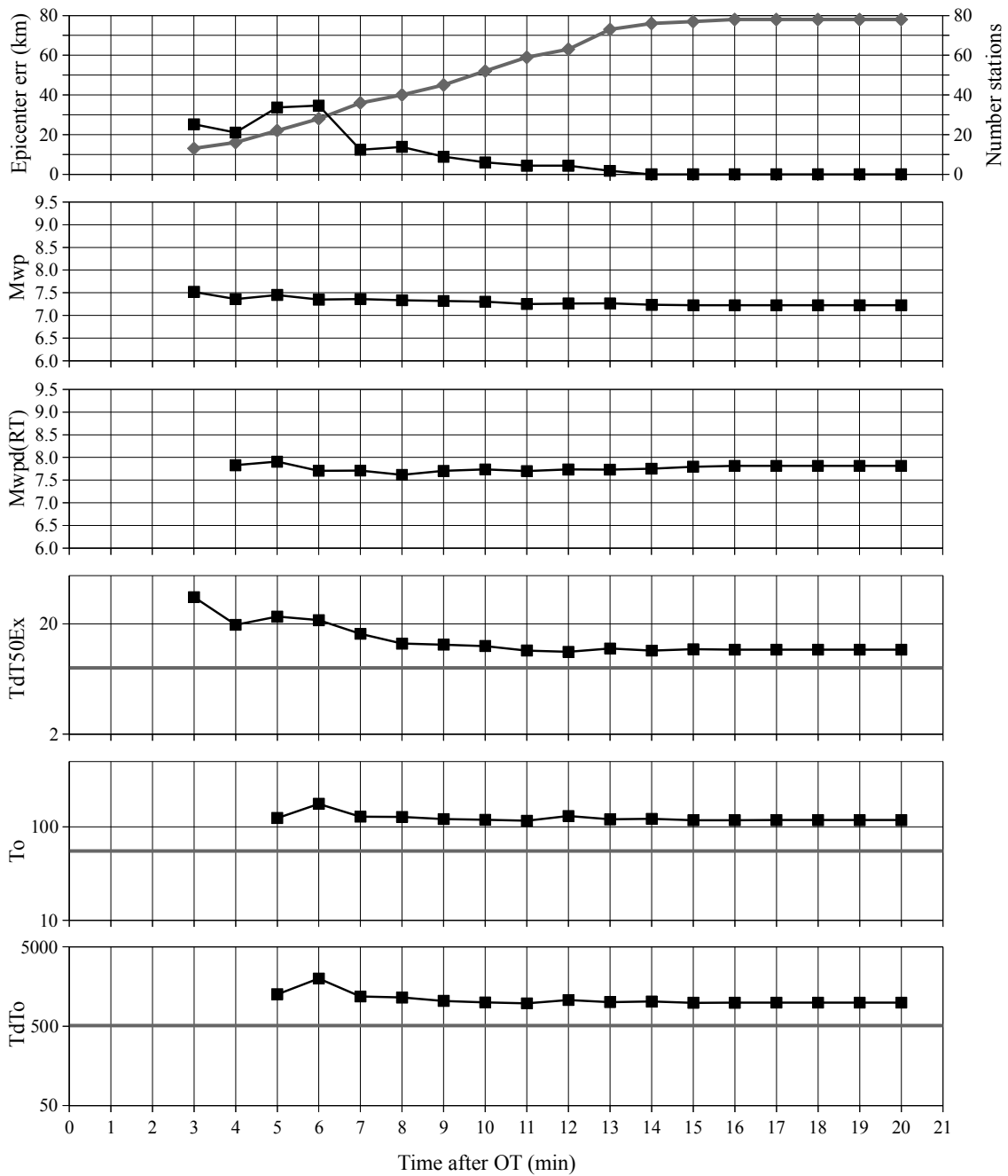


Figure 7

Timeline of event parameter determination for the 2010.10.25, $M_w^{CMT} 7.8$, Mentawai earthquake using the Early-est software and off-line event data. Plot elements as in Figure 5.